Modelling the effects of permafrost thaw and changing hydrology on wetland methane emission from the Northern high latitudes

Mi, Y.

2014

3

Linking Arctic tundra methane emission to sea-ice cover

This chapter up-scales PEATLAND-VU to the Northern high latitudes tundra, and regionally, links the modelled effluxes to the sea-ice cover extent and climatic variables.

Contents

3.1 Introduction . . . 39

3.2 Methods . . . 40

3.3 Results . . . 42

3.3.1 Sea-ice cover trends . . . 42

3.3.2 Correlation of sea-ice cover with CH_4 emission . . . 45

3.3.3 Correlation of CH_4 with climate variables . . . 45

3.4 Discussion . . . 46

3.5 Conclusions . . . 50

3.1 Introduction

Arctic warming promotes changes in CH_4 emission pattern, however, the magnitude is uncertain (Cao et al., 1996, Christensen et al., 1996). Increases in soil temperature can accelerate both methanogenesis, a process that decomposes organic matter and releases CH_4, and CH_4 consumption by microorganism (King et al., 1990, Whalen and Reeburgh, 1990, Yavitt et al., 1988). Besides this, the warming decays permafrost, leading to either increases in CH_4 flux due to the liberation of organic carbon, or decreases due to the improvement of drainage and the consequent lowering of water level (van Huissteden et al., 2011, Vandenberghe et al., 2012).

Changes in precipitation also affect regional hydrology (Frey and Smith, 2003, Rawlins et al., 2010, White et al., 2007). Besides, earlier onset of snowmelt due to elevated air temperature, can lead to a longer growing season, resulting in changes in the rates of photosynthesis and respiration, and therefore the net primary production (NPP) (Aurela et al., 2004, Markus et al., 2009, Shaver et al., 2007). NPP affects methanogenesis by influencing the availability and quality of carbon substrate. Moreover, changes in vegetation composition also plays a key role in CH_4 exchange as vascular plants are more effective conduits for transporting CH_4 from below ground to the atmosphere, and provide fresh carbon substrates (Cadillo-Quiroz et al., 2008, Chasar et al., 2000).

Arctic sea-ice retreat is by and large consisent with Arctic warming over the past decades (Comiso, 2012, Screen and Simmonds, 2010, Serreze and Barry, 2011, Stroeve et al., 2007). Complete ice-free summers are even predicted to occur by the middle of this century (Boe et al., 2009, Josefino et al., 2011, Massonnet et al., 2012, Stroeve et al., 2007, Vancoppenolle et al., 2013). Due to the ice-albedo and ice-insulation feedbacks, shrinking of the sea-ice cover further enhances Arctic warming (Curry et al., 1995, Holland and Bitz, 2003, Lawrence et al., 2008, Serreze and Barry, 2011, Serreze and Francis, 2006).

Parmentier et al. (2013) compared the anomalies in the average Arctic sea-ice extent and the average CH_4 emissions in Arctic wetlands, and concluded that changing sea-ice cover may be connected to the CH_4 exchange between the terrestrial Arctic and the atmosphere. However, the sensitivity of CH_4 exchange to changing sea-ice cover is neither well understood nor quantified, partly due to the complete lack or scarcity of observational data.

This study aims to explore the potential relationships among Arctic climate, sea-ice cover and wetland CH_4 emissions by modelling. In particular, the aim is to link CH_4 emission variations with sea-ice cover retreat within different Arctic regions, which are categorized by the differences in sea-ice extent variations.

The PEATLAND-VU model (Budishchev et al., 2014, Mi et al., 2014b, Petrescu et al., 2010, van Huissteden et al., 2006) is used to simulate CH_4 fluxes from Northern high latitudes.

3.2 Methods

PEATLAND-VU model is employed to simulate circumarctic CH_4 emission from tundra wetlands. Since wetland extension is crucial and may cause large differences between emission estimates (Petrescu et al., 2010), the model is run for three different wetland maps (Fig. 3.1), representing the wetland area percentage in 1×1 degree grid cells. The first map (W1 hereafter) is derived from the GTOPO30 digital elevation model, by assuming that areas with a slope gradient below 1% are likely to support wetlands, as described by van Huissteden (2004). The second one is the wetland map used in Canadell et al. (2011) in the RECCAP project, which is based on Matthews and Fung (1987) (W2 hereafter), and the third one, a wetland map developed by Kaplan (2002) (W3 hereafter).

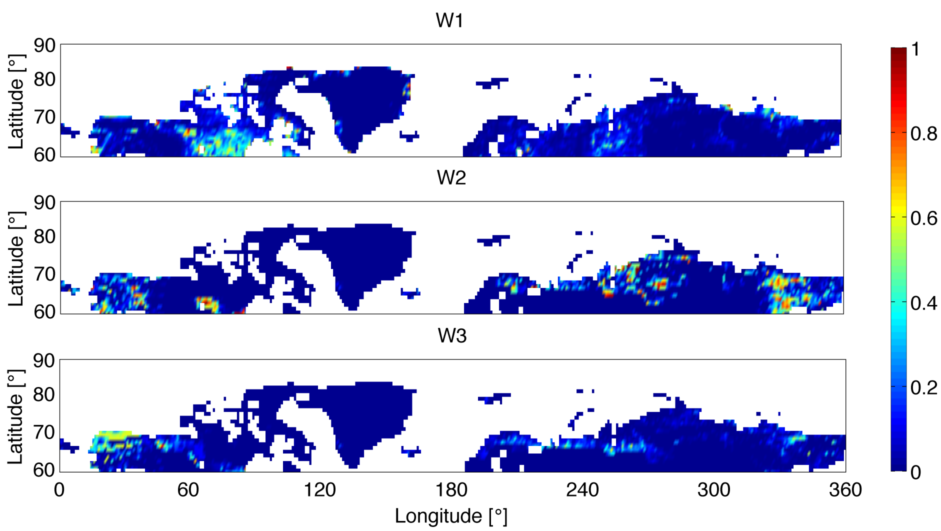

Figure 3.1: Three wetland maps

W1 is based on digital elevation model of GTOPO30, which delineates all areas having potentially poor drainage due to flat topography as wetlands. This method may not be accurate in the areas affected largely by glaciation, which created much small-scale relief and not well represented in the GTOPO30 data. Also the areas have a lot bare rock outcrops tend to be flat, which could be mistaken as wetlands. Therefore W1 overestimates the wetland areas in

Canadian Shield and Greenland. W2 and W3 are derived from worldwide topographical maps and satellite datasets. Areas that do not show up as wetlands in these data, such as the west Siberian lowland, could still have saturated soils for part of the year and thus have CH_4 emissions. Therefore from the perspective of CH_4 emission modelling, these areas should be included. In particular, when applying Peatland-VU, which contains a module to calculate water table, W1 should be considered as the upper limit of the wetland area.

For each grid cell, the model is parametrized separately for peatland, floodplain soils and other wetland soils (tundra gley soils)(Fig. 3.2). The latter two are parametrized as fine-grained mineral soils with an organic horizon that is too thin to classify as histosol. Although the floodplain soils comprise a relatively small area, they may show high CH_4 fluxes, as shown by van Huissteden et al. (2005), therefore are modelled separately. The organic horizon thickness in these soils has been taken as 0.4 m, while for peat soils the entire soil column (1.5 m) is taken to consist of peat. The mineral horizons below the organic topsoil of the gley and floodplain soils are assumed to consist of fine-grained material. For all soils a 0.2 m thickness of low bulk density topsoil has been assumed (acrotelm). For calculating the soil temperature profile, the lower boundary of the profile is set at 20 m below the surface; the lowest horizon in the profile is assumed to extend to this depth, except for peat soils where a transition between peat and mineral material is assumed to occur at 2 m depth.

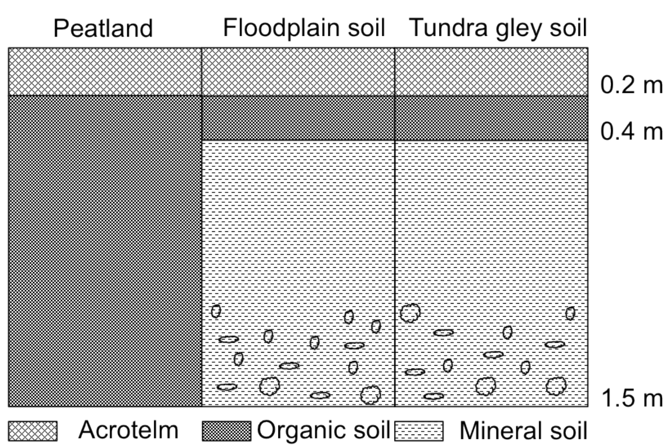

Figure 3.2: Soil profile parametrized in the model.

The soil classes have been derived from the FAO/UNESCO world soil map (FAO/IIASA/ISRIC/ISSCAS/JRC, 2012), while the tundra area has been delineated using the Biomes of the World map (de Blij and Muller, 1995). Climate data input for the model consists of daily mean air temperature, snow cover thickness, daily precipitation and evaporation and snow meltwater production, derived from the ERA-Interim reanalysis, `http://www.ecmwf.int/research/era/do/get/era-interim` (Dee et al., 2011). For each model grid cell, the data have been selected that are located closest to the centre. The model has been run with a two-year spin-up. The modelling framework calculates an area-weighted average flux over all three soil types for each grid cell. The model domain includes all tundra areas over a 60-80 degree latitude band. The analysis is restricted to the tundra biome, as this is assumed to have the strongest maritime influence of Arctic biomes (Bhatt et al., 2010, CAVM Team, 2003).

For further analysis, CH_4 fluxes, driving climate variables, and sea ice cover percentage are averaged in 60 degrees wide sectors across the Arctic (Alaska, -180°- -120°, Canada, -120°- -60°, Greenland -60°- 0°, Europe 0°- 60°, Western Siberia 60°- 120°, Eastern Siberia 120°- 180°). The sea-ice cover data are obtained from the National Snow and Ice Data Center (NSIDC) (Fetterer et al., 2002, updated daily). The sea-ice cover extent of Septembers (1981-2010) are used in this study. Parmentier et al. (2013) used the sea-ice coverage of growing season average in their study. Comparison of these two datasets shows that they are highly correlated. The CH_4 fluxes and climate variables are area weighted based on sector wetland area.

Panels in Fig. 3.3 display the modelled annual average CH_4 fluxes. W1 shows higher emissions from the Canada sector, while W2 has high emissions from the Siberia sectors. The differences in CH_4 emissions are an effect of the large differences between the wetland maps. Beside the overestimation of wetland area in Canadian Shield by W1, W2 shows high wetland fraction grid cells that line up along the rivers. These areas are configured as high emission floodplain soils in our model, which amplifies the fluxes.

3.3 Results

3.3.1 Sea-ice cover trends

Linear regressions of the sea-ice cover against time show a significant ($p<0.05$) decrease in all six sectors except the Europe sector (Fig. 3.4). Changes are the strongest in the Alaska and East Siberia sectors, -0.29% and -0.27% per year, respectively.

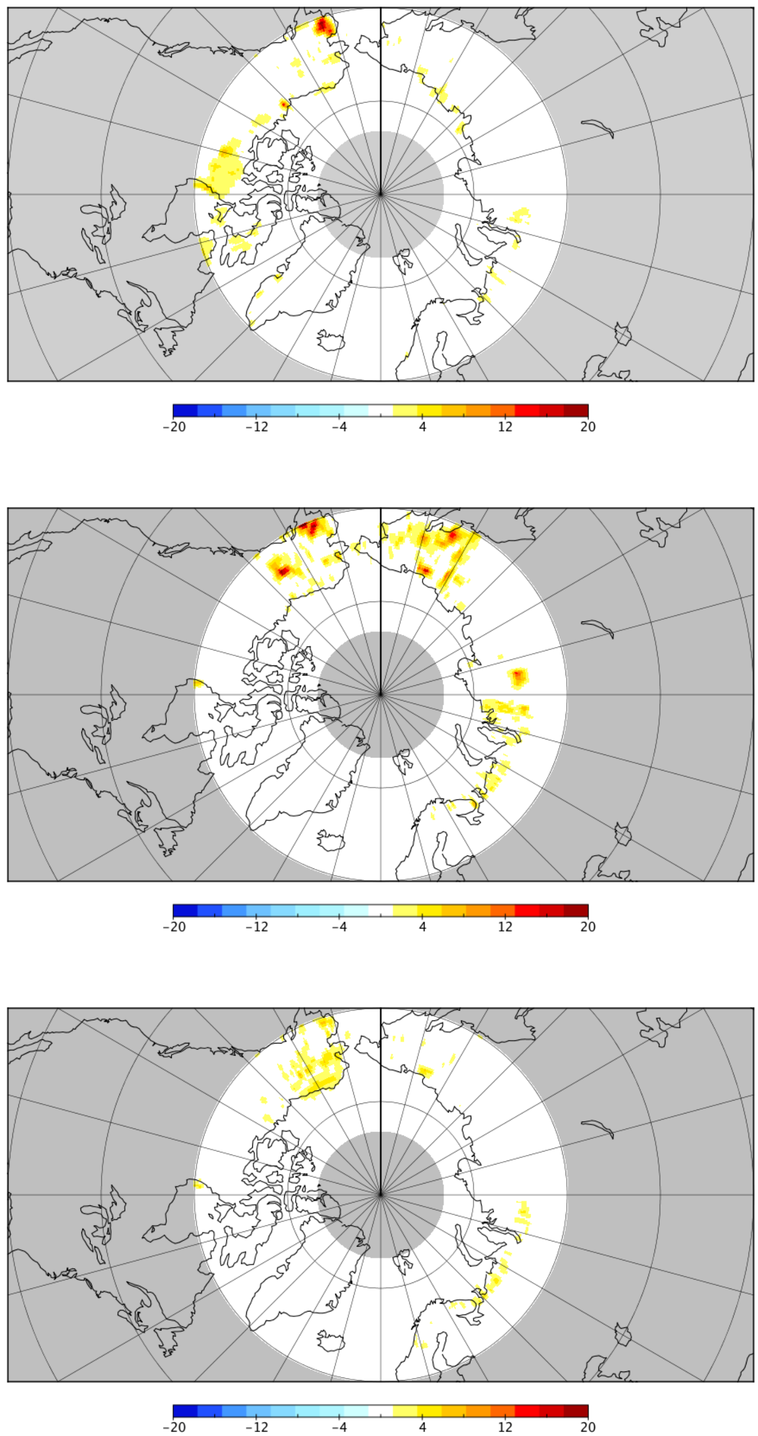

Figure 3.3: Modelled annual average CH_4 fluxes ($mg \cdot m^{-2} \cdot hr^{-1}$) for wetland configuration W1 (above), W2 (middle) and W3 (below).

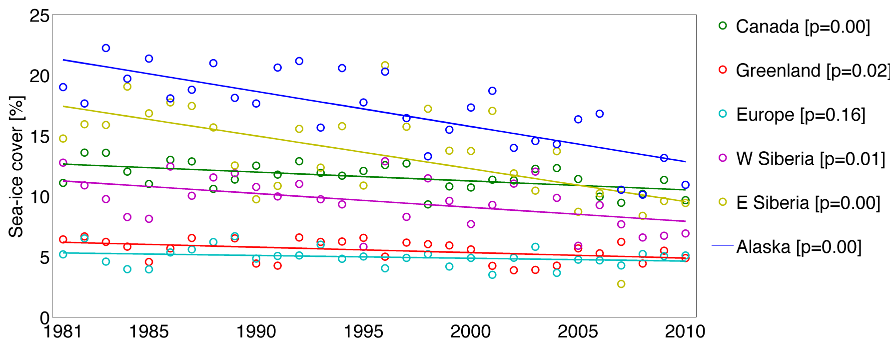

Figure 3.4: Linear regressions of sea-ice cover for six sectors, 1981-2010.

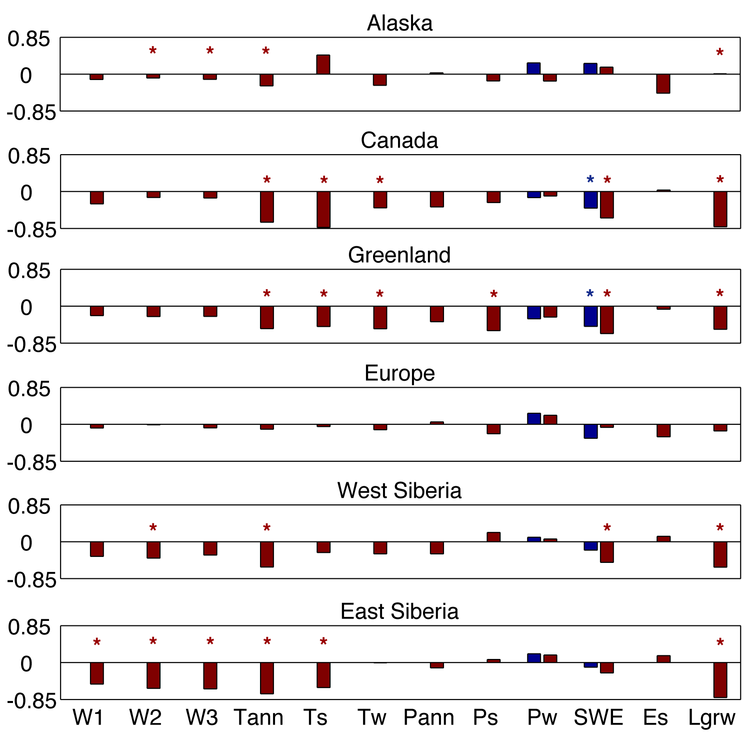

Figure 3.5: Correlations of sea-ice cover extent with CH_4 emissions and climatic element. The sea-ice cover is presented for both previous year (Blue) and present year (Red). W1, W2 and W3 denote simulated CH_4 emissions from three wetland map configurations, respectively. T_{ann}, annual air temperature, T_s, summer air temperature, T_w, winter air temperature, P_{ann}, annual precipitation, P_s, summer precipitation, P_w, winter precipitation, SWE, snowmelt water, E_s, summer evaporation, L_{grw}, growing season length. The stars denote the correlations have passed the significance level of p=0.05.

3.3.2 Correlation of sea-ice cover with CH_4 emission

Potentially, sea-ice retreat may cause elevated CH_4 emissions in these regions by its effects on local climate and the consequential changes in soil temperature and hydrology. The sea-ice cover and CH_4 emissions are significantly ($p<0.05$) correlated in the Alaska and East Siberia sectors (Fig. 3.5). These regions are underlain by permafrost and have extensive wetlands coverage. The correlation strength may vary among the three wetland configurations, for instance the correlation is significantly strong for all three configurations in the East Siberia sector, for W2 and W3 in the Alaska sector and for W2 only in the West Siberia sector. In contrast, no significant correlations are found in the Canada, Greenland and Europe sectors. However in the European and Greenland sectors, CH_4 emissions correlate significantly with previous year's ice cover.

Sea-ice cover is strongly correlated with air temperature, mainly annual and summer air temperature. Correlation with precipitation is less clear except for Greenland. However, the correlation in Greenland may be spurious due to the small coverage of wetlands. The sea-ice cover is also significantly linked to growing season length and spring snowmelt water, which are both substantially related to air temperature. However, the correlation for the Europe sector is not significant for any climatic element.

The correlations of the winter precipitation and the snowmelt water with the ice-cover of previous years have been further checked, as they could be affected due to the effect of an open Arctic ocean on moisture (Francis and Hunter, 2007, Graversen and Wang, 2009). However, this effect is not clear on the winter precipitation, and the negative correlations with snowmelt water are significant in Canada and Greenland sectors.

3.3.3 Correlation of CH_4 with climate variables

Correlations of CH_4 emission with climate variables (Fig. 3.6) generally follow the processes that are included in the PEATLAND-VU. Next to air temperature and growing season length, modelled CH_4 emissions also correlate with climate variables related to soil hydrology such as annual and summer precipitation, and snowmelt runoff.

However, the climatic drivers of CH_4 emissions differ among sectors. The emissions are primarily driven by air temperature in the Europe and Siberia sectors, whereas precipitation is more important in the Alaska and Canada sectors. Besides, emissions from the Alaska and East Siberia sectors are also strongly influenced by growing season length, while in Greenland and Europe sectors, spring snowmelt water plays an important role. This is consistent with the thicker snow cover that is found in these areas compared to other sectors.

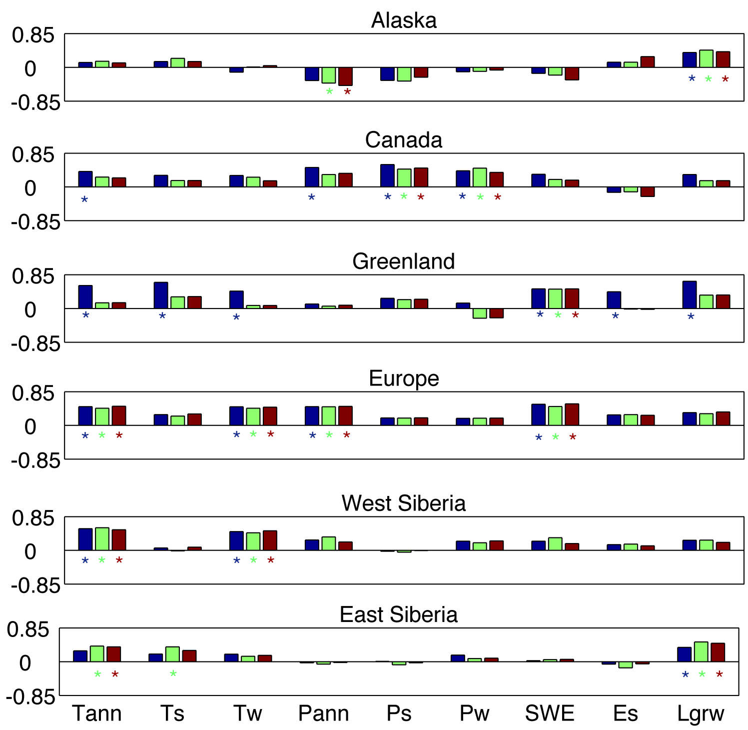

Figure 3.6: Correlations of CH_4 emissions with climatic variables for three wetland map configurations (Blue-W1, Green-W2, Red-W3). T_{ann}, annual air temperature, T_s, summer air temperature, T_w, winter air temperature, P_{ann}, annual precipitation, P_s, summer precipitation, P_w, winter precipitation, SWE, snowmelt water, E_s, summer evaporation, L_{grw}, growing season length. The stars denote the correlations have passed the significance level of p=0.05.

The negative correlations of air temperature with the previous year sea-ice cover in most cases suggest that low sea-ice cover leads to high air temperatures. However, the positive correlation in Alaska sector indicates that a warm summer may follow a year with large sea-ice covered. Therefore, the question remains whether declines in sea-ice cover cause higher air temperature or vice versa.

3.4 Discussion

It is difficult to demonstrate causal relationships between sea-ice decline and processes on land. The Arctic amplification is a complex of forcings and feedbacks, causing enhanced warming of the Arctic with respect to lower latitudes.

Acting together with a warming by inflowing Atlantic and Pacific ocean water (Bourgain and Gascard, 2011), the exact role of a decrease of sea-ice extent and ice-albedo effect in the Arctic amplification has been subject to debate. Chung and Räisänen (2011) demonstrate that snow-ice-albedo feedbacks at least enhance the effects of longer distance heat transport. Graversen and Wang (2009) argued that the role of sea-ice decline is minor while others consider it a main factor (Screen and Simmonds, 2010). Besides sea-ice decline, increased water vapour and clouds may also play a role in the Arctic amplification (Francis and Hunter, 2007, Graversen and Wang, 2009). However, with a global circulation model study, Screen and Simmonds (2010) have shown that long distance transport of heat from lower latitudes mostly affects temperatures in the upper Arctic atmosphere, while 50-75% of temperature change at the surface could be explained by sea-ice decline. This implies that sea-ice decline has a strong impact on temperature-dependent processes in Arctic soils, such as CH_4 formation.

Some data and model simulations show the effects of sea-ice decline on land. The highest warming of the terrestrial environment is seen to be at distances up to a few hundred kilometers off the Arctic coast (Bekryaev et al., 2010). Lawrence et al. (2008) demonstrated that the warming signal may penetrate up to 1500 kilometers inland and may affect permafrost stability. Parmentier et al. (2013) therefore argue for a relation between decreasing sea-ice extent and terrestrial CH_4 fluxes in the Arctic, suggesting a teleconnection between the two.

Our modelling work confirms this increase in the CH_4 fluxes, and moreover, demonstrates that this is not evenly distributed. The strongest effects are found in the East Siberian and Alaskan sectors of the Arctic, with the fastest rate of sea-ice decline. These are the same areas with extensive vulnerable permafrost carbon stores, and with the ice-complex (yedoma) deposits (e.g. Zimov, 2006). In these areas, correlations between sea-ice decline and terrestrial CH_4 fluxes are also significant.

A smaller rate of sea-ice decline is seen in the West Siberian and Canadian sectors. In the Canadian sector, the correlations between sea-ice area and CH_4 flux are not significant, although the relations are quite strong; in the West Siberian sector these correlations are significant. A higher wetland percentage in the West Siberian sector may have caused a stronger effect. In the Greenland and European sectors, the sea-ice decline is smaller, and there is no correlation with CH_4 and sea-ice area. Here, the effect of warming is largely governed by oceanic heat transport, and in these sectors the wetland percentage is small.

Except in the European sector where sea-ice decline is the weakest, significant correlations of sea-ice extent with annual and summer air temperature are found; in Canada and Greenland also with winter air temperature. By contrast, the correlations with precipitation are weaker and less consistent. Only for Greenland a strong negative correlation with summer precipitation is present, suggesting that a lower sea ice cover causes more summer precipitation. In most sectors, strong correlations with growing season and spring snowmelt can also be seen, which are largely an indirect temperature effect.

Despite clear correlations of CH_4 with air temperature, correlations between ice-cover and precipitation are largely absent. Therefore I conclude that the effect of ice-cover on temperature operates largely through warming of the air over the tundra and subsequent warming of the soil. This warming effect feeds back on CH_4 emissions through different pathways in the four extensive wetland sectors. In Alaska, the linkage is the length of growing season, whereas in West Siberia, it is the air temperature; and in East Siberia, both are active. CH_4 emissions from the Canada sector are constrained by precipitation, on which sea-ice cover has no direct effect.

It should be noted that our model does not include the physical effects of permafrost thaw. Localized thawing of ground ice causing the terrain depressions with a high water table and the formation of ponds and lakes, may enhance CH_4 emission considerably (Backstrand et al., 2010, Turetsky et al., 2008). In this study, only the effects of soil temperature and water table are considered. Therefore the simulations are likely to underestimate the effect of sea-ice decline on terrestrial wetland CH_4 emissions as this additional source of methane is not included in the model.

The modelled annual emissions are compared with that of an inverse model results by Houweling et al. (2014) (Fig. 3.7), in which the TM5 4DVAR inverse modelling system has been used to retrieve CH_4 emissions from the SCIAMACHY satellite data. The systematic errors of the retrievals are corrected by the measurements from the Total Carbon Column Observing Network (TCCON). The model simulations configured by W2 for sector Canada and Greenland are used, as W1 overestimates the wetland coverage in Canadian Shield and Greenland, and W1 for the rest to calculate the total emissions within each sector. The magnitudes of these two datasets are comparable, but the interannual variability is inconsistent.

There are no long-term ground-based observation datasets on Arctic wetland CH_4 fluxes that may be used to test the effect of ice-cover as modelled here, and the existing datasets are measured by various methods and may consist gaps. The data presented by Backstrand et al. (2010) from the Stordalen mire in Northern Sweden go back to 1970, but focuses on the years 2002-2007. The authors note a clear increase in the emission of total hydrocarbon gases (mainly CH_4). Backstrand et al. (2010) attribute the increase to environmental

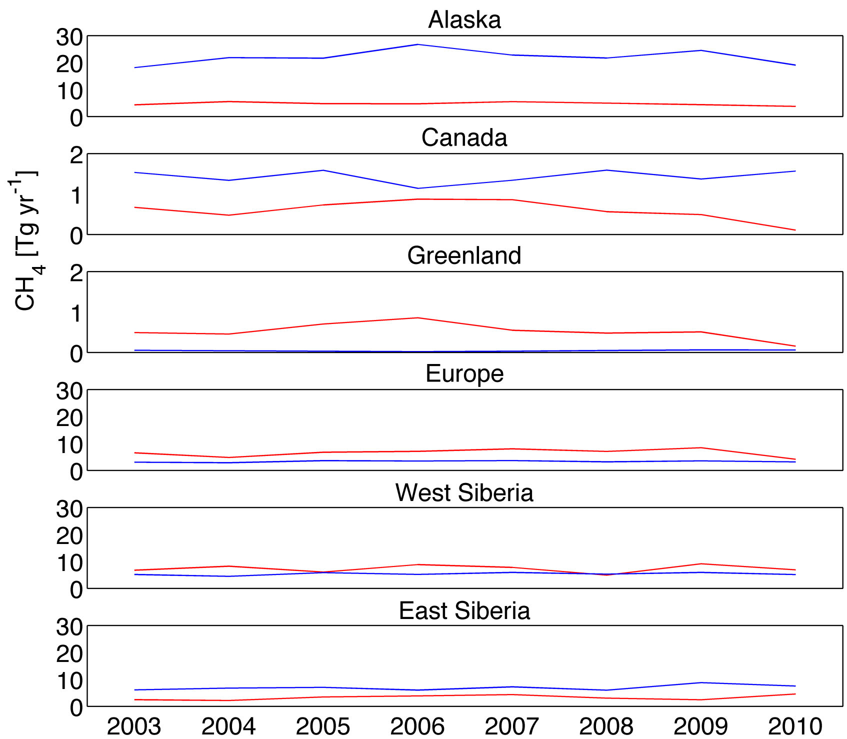

Figure 3.7: PEATLAND-VU simulations (Blue) compared with inverse model retrievals from SCIAMACHY sitellite data (Red).

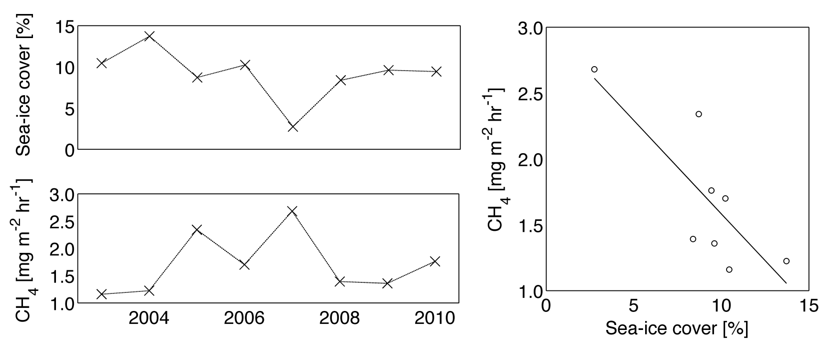

Figure 3.8: The yearly average CH_4 fluxes modelled by PEATLAND-VU on Kytalyk site, Northeastern Siberia, and the corresponding sea-ice cover percentage in East Siberia sector, 2003-2010.

change by ground ice thaw resulting in palsa collapse, which is not included in our model. This site is located in the European sector, where no clear direct indications of correlation of CH_4 emissions with ice-cover were found, although an indirect effect of ice cover from previous years may be present. Another site with a longer-term data set is the Kytalyk research site in Eastern Siberia with data from 2003-2013. However, the first 4 years of data from this site consist of very short periods of flux chamber measurements. Mi et al. (2014b) modelled the fluxes with PEATLAND-VU constrained by the data and based on local weather observations. These data clearly reflects the influence of sea-ice cover extent on CH_4 fluxes; the record low sea-ice minimum of 2007 is represented by a higher flux (Fig. 3.8). Linear regression of the CH_4 emissions on sea-ice cover extent gives a coefficient of determination (R^2) value of 0.63 ($p=0.02$). This essentially confirms our model results.

3.5 Conclusions

In this study, the pan Arctic regions are divided into six sectors, and link the sea-ice cover extent with modelled CH_4 emissions from the wetlands within each sector. Their relationships with climatic elements have been further analyzed. The decrease rates of sea-ice cover are the fastest in the Alaska and East Siberia sectors. Increases in CH_4 emissions in these regions are significantly correlated with sea-ice cover, where the same areas are underlain by carbon-rich permafrost and with extensive wetland coverage. Furthermore, the sea-ice cover is strongly correlated with air temperature, and less with precipitation. CH_4 emissions are correlated with climatic variables, in the descending order of air temperature, growing season length, and hydrology related variables. Comparison of modelled CH_4 emissions from a Northeastern Siberian tundra site with sea-ice cover of the same section confirms the close correlation between them.